Earthquakes and Structures, *Vol. 16, No. 3 (2019) 253-263*
DOI: https://doi.org/10.12989/eas.2019.16.3.253

Rehabilitation of exterior RC beam-column connections using epoxy resin injection and galvanized steel wire mesh

Comingstarful Marthong*

Department of Civil Engineering, National Institute of Technology Meghalaya, Shillong 793003, India

(Received October 24, 2018, Revised January 3, 2019, Accepted January 4, 2019)

Abstract. The efficacy of a galvanized steel wire mesh (GSWM) as an alternative material for the rehabilitation of RC beam-column connections damaged due to reversed cyclic loading was investigated. The repair mainly uses epoxy resin infused under pressure into the damaged zone and then confined using three types of locally available GSWM mesh. The mesh types used herein are (a) Weave type square mesh with 2mm grid opening (GWSM-1) (b) Twisted wire mesh with hexagonal opening of 15 mm (GSWM-2) and (c) welded wire mesh with square opening of 25 mm (GSWM-3). A reduced scale RC beam-column connection detailed as per ductile detailing codes of Indian Standard was considered for the experimental investigation. The rehabilitated specimens were also subjected to similar cyclic displacement. Important parameters related to seismic capacity such as strength, stiffness degradation, energy dissipation, and ductility were evaluated. The rehabilitated connections exhibited equal or better performance and hence the adopted rehabilitation strategies could be considered as satisfactory. Confinement of damaged region using GSWM-1 significantly enhanced the seismic capacity of the connections.

Keywords: beam-column connections; rehabilitation; Epoxy resin injection; galvanized steel wire mesh; seismic capacity

1. Introduction

Beam-column connections comprises of the joint plus the columns, beams, and slab adjacent to the joint (ACI 352R-02 2002). Beam-column connections may be classified into three types viz. exterior joint, interior joint and corner joint. The behavior of these RC beam-column connections plays an important role in the response of a framed structure. It is the weakest link of the frame structures (Silva and Haach 2016). However, it strongly influences the seismic behavior and energy dissipation capacities of the moment resisting frames. In the past, numerous reinforced concrete frame structures collapsed due to severe earthquake. Post-earthquake investigations into damaged structures generally showed that in many cases, damages of RC frame structure were localized in beam-column connections which might have led to partial or total collapse of the building. Further, it was observed that the exterior beam-column connections had suffered more in comparison to the interior ones. The failure of these connections during past earthquakes opened a new research direction in the field of repair of damaged structures. Research in this area is essential as engineers in seismic-prone regions often face the task of analyzing and designing repairing works for damaged buildings. Thus, it is difficult to decide always whether to discard the damaged structure or to rehabilitate the same for retrieving the lost capacity without any quantitative guidance. After any major earthquake, there is a general concern on the issue of deciding the strategy of effective and reasonable rehabilitation of damaged structures for post-earthquake usage. However, in most cases, severely damaged structures are thought to be irreparable and are abandoned in spite of huge economic loss. Thus, to ensure further usability of the damaged structure effective rehabilitation methodology need to be investigated.

2. Rehabilitation techniques

Rehabilitation is aimed at repairing of damaged structural components. The scope of repairs for individual structural element depends on the objectives of the repair program. A number of studies have addressed the repair of RC components damaged as a result of earthquake events. Application of repair techniques after damaging the beam-column connection provided information regarding the effectiveness of the repair. Tsai (1992), Filiatrault *et al*. (1996), Tsonos and Papanikolaou (2003), Kakaletsis *et al*. (2011), Marthong *et al*. (2013) described the improvement of the behavior of the connection after injection of epoxy resin at cracked region. Karayannis *et al*. (1998) prescribed properties of the cementitious material for patching of spalled and crushed concrete. FEMA 308 (1998) and ACI 546-96 (1996) were used by many researchers as a basis for defining and validating repair method. Application of shotcrete jacketing (Tsonos 2010), thin RC jacket (Karayannis *et al*. 2008), lap splice (Kalogeropoulosa and Tsonos 2014) were experimentally investigated and found effective in restoring and enhancement the seismic capacity of beam-column connections. Several techniques for

*Corresponding author, Associate Professor
E-mail: commarthong@nitm.ac.in

http://www.techno-press.com/journals/eas&subpage=7
ISSN: 2092-7614 (Print), 2092-7622 (Online)

rehabilitation and strengthening of damaged connections were reported by Engindeniz *et al*. (2005). Of the various techniques, the most commonly used were jacketing with concrete and steel. These techniques possess its own practical limitations like labour intensive, artful detailing, increased dimension of structural element, susceptibility to corrosion etc. The use of epoxy-bonded FRP sheets or strips as confining materials for repair or strengthening of RC beam-column connection has been reported by various researchers (Mosallam 2000, Ghobarah and said 2002, Karayannis and Sirkelis 2002, Mukherjee and Joshi 2005, Karayannis *et al*. 2008, Tsonos 2008, Saleh *et al*. 2010, Alsayed *et al*. 2010, Eslami and Ronagh 2014, Tsonos 2014, Hadi and Tran 2016, Ascione *et al*. 2017). They showed that seismic capacity and failure modes of the RC beam-column connections significantly improved. However, the effectiveness of any rehabilitation/strengthening techniques depends on the treatment provided to the fragmented concrete in the damaged region (Corazao and Durrani 1989, FEMA 308 1998, Karayannis 1998, Karayannis *et al*. 2008, Marthong *et al*, 2013). Hence, in this study an effort shall be focus on rehabilitating the affected damage zone. As mentioned FRP are commonly used for rehabilitation and strengthening of beam-column connections and has been proved that seismic capacity significantly enhanced. Although the use of FRP jackets enhanced the joints seismic performance, anchoring of FRP materials has evolved as a difficult problem for the effectiveness of this technique (Ghobarah *et al*. 1997). Researchers also observed different types of failure that reduced the performance of FRP rehabilitated structural elements (Esfahani *et al*. 2007, Teng *et al*. 2002). These failures are often brittle and include debonding of FRP. Thus, it is necessary to investigate an alternative wrapping material for FRP, which is more ductile and have better bond characteristic. In addition to FRP, stainless steel wire mesh composite (Choi 2008, Li *et al*. 2015, Bansal *et al*. 2016, Kumar and Patel 2016, Patel *et al*. 2018), composite grid (Bentayeb *et al*. 2008) and geo-grid confinement (Chidambaran and Agarwal 2014) have also been investigated as strengthening methods to improve strength and ductility of RC structural elements. However, owing to the high manufacturing and application costs of these materials, the need has arisen to investigate other possible wrapping materials.

In this paper a relatively cheap materials i.e galvanized steel welded wire mesh (GSWM) locally available in the market was used to confine the damaged zone of RC beam-column connections. The advantages of GSWM are high tensile strength, low weight, corrosion resistance, minimum change in geometry, rapid installation process and cost effective. GSWM serve as an external reinforcement which can be glued to the concrete surface using epoxy or cement mortar and hence increase the bond resistance.

3. Experimental program

3.1 Selection of RC beam-column connections

A free body diagram of an isolated exterior beam-column connection in its deformed position is shown in Fig. 1. It comprises of half height of a column at top and bottom as well as half of a beam length, which corresponded to the points of contra-flexure in beam and column under lateral loads. In this figure, h_c is the story height, l_b is half beam span corresponding to the length of the beam connected to the selected joint, N is the internal axial force of the column, P is the beam-tip load, V_{col} *is* the column shear force and Δ is the vertical beam-tip displacement. It may be noted that the symmetric boundary condition were maintained at both the ends of column for isolation of a single unit of beam-column connection. In this study, a typical full scale residential building with floor to floor height of 3.3 meters and the beam effective span of 3.0 meters were considered. The dimension of beam and column was chosen as 360 mm×450 mm and 360 mm×360 mm respectively. A 20 mm diameter high yield strength deformed (HYSD) bar was used for both beam and column as main reinforcement. Cross section analysis was based on the equilibrium equation and the moment carrying capacity of beam and column was calculated as 94.57 kN-m and 112.62 kN-m. The ratios of column-to-beam flexural capacity satisfy the criteria of strong column-weak beam condition (IS 13920-2016, ACI 318). The beam-column connection was scaled down to one-third size for experimental investigation. Reinforcement and coarse aggregates were also geometrically scaled down for satisfying the similitude requirement.

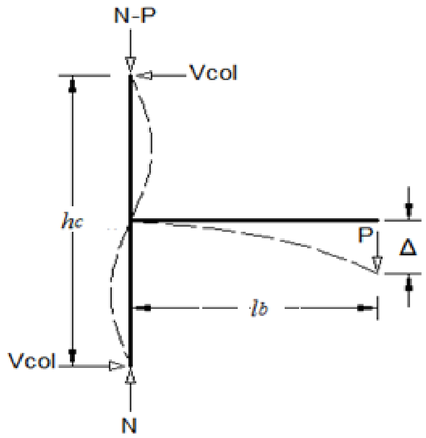

Fig. 1 Isolated exterior beam-column connection

3.2 Description of RC beam-column connections

The detailed description of one-third size exterior RC beam-column specimen is presented in Table 1. Following the standard code of practice (IS 13920-2016, IS 456-2000) the beam specimen was designed as under reinforced section. A cross section of 120 mm×120 mm and 120 mm×150 mm for column and beam elements respectively were considered. HYSD bars of 8 mm diameter (Fe 500) were used as main bars in both column and beam. Following the code provision of IS 13920 (2016) a lateral tie of 6 mm diameter mild steel bars (Fe 250) at 25 mm c/c spacing was used in the special confinement zone of the column, while the remaining part was increased to 50 mm c/c. Similarly, the shear reinforcement in beam was of 6 mm

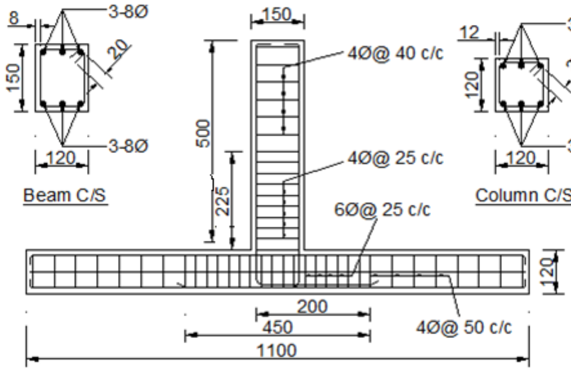

(All dimensions are in mm)

Fig. 2 Reinforcement detailing of beam-column specimens

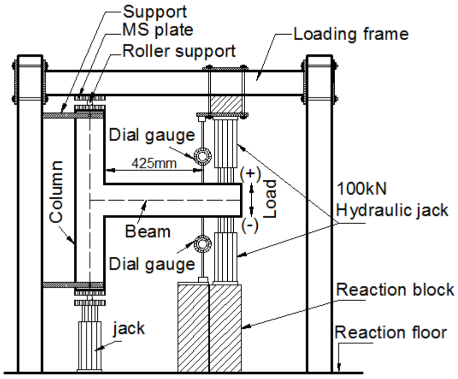

(a)

(b)

Fig. 3 Testing of beam-column connection (a) Test set-up (b) Actual testing arrangement

diameter bar having spacing of 25 mm c/c near the beam-column joint for a length of 225 mm and a spacing of 40 mm c/c in the remaining part. The yield stress (N/mm^2) and ultimate stress (N/mm^2) for HYSD bars tested as per code provisions (IS 432 (I)-1982, IS 1608-1995) were found out to be 530 N/mm^2 and 620 N/mm^2, while the same for Fe 250 were 285 N/mm^2 and 450 N/mm^2 respectively. The detailing of the specimen is shown in Fig. 2.

3.3 Casting of RC beam-column connections

Three exterior RC beam-column specimens were casted. The concrete mix was designed for a characteristic cube compressive strength of 25 N/mm^2 which resulted in a target mean cube compressive strength of 31.6 N/mm^2 as per IS 10262 (2009). All concrete mixes were produced with 383 kg/m^3 of cement, 720 kg/m^3 of fine aggregate, 1100 kg/m^3 of coarse aggregate, for a water-cement ratio of 0.5 and a compaction factor of 0.9. Cement concrete cubes 150 mm×150 mm×150 mm were casted for compressive strength determination. Specimens were demoulded after 24 hours of casting and were kept in the water tank for 28 days curing period. The compressive strength after 28 days was recorded as 33.16 N/mm^2. The beam-column connections were designated as S2, S3 and S4. All these specimens were treated as a control specimen and subjected to reverse cyclic loading.

3.4 Test set-up and instrumentation

Fig. 3 shows the setting of the test set-up and the actual testing arrangement. For applying the load to the specimens, a loading frame of 500 kN capacity and hydraulic jack of 100 kN were used. In the testing frame, the column was positioned vertically while the beam is placed horizontally. To represent the gravity load, an axial load using hydraulic jack was applied to the column. The moments were approximately zero at the mid-span of the column when subjected to lateral loading. To model the actual conditions of zero moments, roller supports were provided at both ends of the column. The cyclic loading was applied manually at a distance of 100 mm from the free end of the beam by mean of two hydraulic jack mounted at the top and at the bottom. The 100 kN capacity hydraulic jack was well equipped with an in-built manually operated pumping units fitted with bourdon tube type load gauge and high-pressure flexible hose pipe. To measure the vertical displacement of the beam, two 100 mm measuring range dial gauges were placed at the top and bottom face of the beam tip.

3.5 Loading sequence

In the present study, the loading sequence suggested by Vidjeapriya and Jaya (2013) is adopted. A displacement controlled mode was applied to the specimens. However, instead of three cycles at every amplitude of displacement one loading cycle was considered. The loading history is presented in Fig. 4. A maximum displacement of ±30 mm was applied in all the specimens.

In order to utilize results obtained from cyclic loading test on structural elements for a general performance evaluation, there is a need to establish loading history that captures the critical issues of the element capacity as well as the seismic demand. The importance of loading sequence effects has not yet been established through research, and the sequence of large vs. small excursions in an element of a structure subjected to a severe earthquake does not follow any consistent pattern (Karayannis and Sirkelis 2008). In the adopted loading, emphasis was given on the large inelastic excursion since they caused large damage and could lead quickly to ultimate state.

The ratio of beam tip displacement to the length of the beam measured from the joint to the position of the dial

Table 1 Descriptions of beam-column connections

Beam			Column			$M_R = \frac{\Sigma M_C}{\Sigma M_B}$
Span (mm)	Section (mm×mm)	Longitudinal Reinforcement	Length (mm)	Section (mm×mm)	Longitudinal Reinforcement	
500	120×150	3-8ϕ-top 3-8ϕ-bottom	1100	120×120	3-8ϕ+3-8ϕ-total	2.38

M_R: ratio of column-to-beam flexural capacity
ΣM_C: sum of flexural capacities of the columns meeting at the joint under consideration
ΣM_B: sum of flexural capacities of beams at the same joint

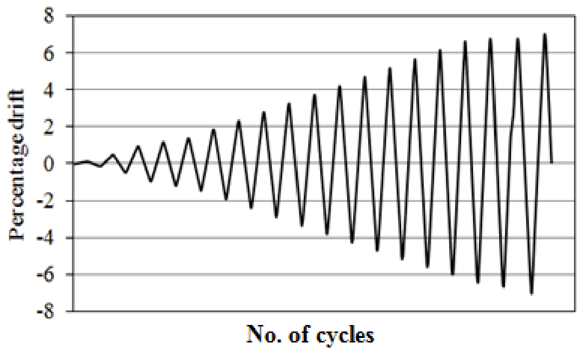

Fig. 4 Loading history

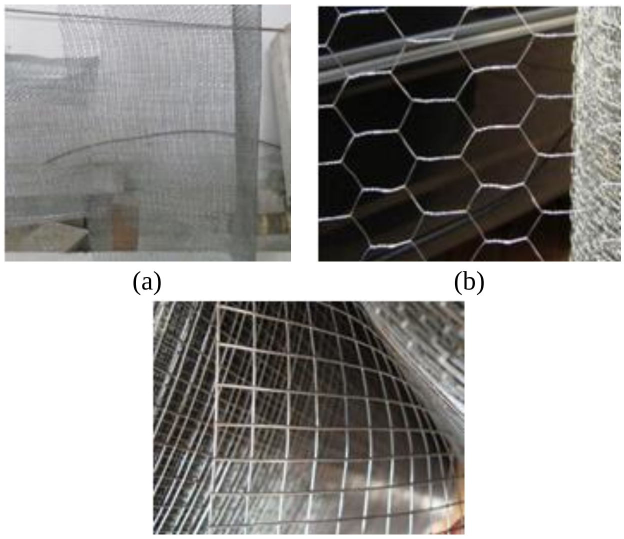

(a) (b) (c)

Fig. 5 Mesh types (a) GSWM-1 (b) GSWM-2 (c) GSWM-3

Table 2 Properties of epoxy resin, micro-concrete, bonding agent, sealing material

Materials	Properies	Value
Epoxy resin	Density	approx.. 1050 kg/m^3
	Tensile strength	26 N/mm^2@7days
	Flexural strength	63 N/mm^2@7days
	Compressive strength	93 N/mm^2@7days
Micro-concrete	Compressive strength	40 N/mm^2@7days
	Tensile strength	2.0 N/mm^2@28days
	Flexural strength	5.0 N/mm^2@28days
Bonding agent	Compressive	50 N/mm^2@7days
	Tensile strength	26 N/mm^2@7days
	Compressive strength	50 N/mm^2@7days

gauge is called the drift angle. Drift obtained by horizontally displacing the beam ends are equivalent to the inter-storey drift angle of a structure subjected to lateral loads. Two hydraulic jacks were mounted on top and bottom of the beam tip end to apply the reversed cyclic loading. As suggested by Ghobarah *et al*. (1997), an axial load of 10% of the gross capacity of the column was applied to the column end by utilizing a hydraulic jack to represent the dead load transferred from upper floors.

3.6 Materials / equipment for rehabilitation

The materials used for repairing the damaged control specimens are low viscous epoxy resin (Conbextra EP10), micro concrete (Renderoc RG), concrete bonding agent (Nitobond EP) and Sealant material (Nitocote VF). All these materials were procured from Fosroc Chemicals (India) Pvt. Ltd.. The properties obtained from the data sheet supplied by the manufacturer are presented in Table 2. Further, an injection pumps (hand operated) suitable for the injection of low viscous resins up to an injection pressure of 100 bar. Mechanical packers (type S, length of 70 mm and dia. of 13 mm) are used in the repairing works. The packers are drill-hole packers which are screwed into the drill-holes. When tightening the packers a fabric-reinforced rubber sleeve and firmly pressed against the drill-hole sides so that the packers can withstand even highest injection pressures in the drill-hole.

Locally available galvanized steel wire mesh (GSWM) of three grid opening size and weaving types as shown in Fig. 5 were used in the present study. These materials are (a) Weave type square mesh with 2 mm grid opening (GWSM-1) (b) Twisted wire mesh with hexagonal opening of 15 mm (GSWM-2) and (c) welded wire mesh with square opening of 25mm (GSWM-3). The diameter of wires in GSWM-1, GSWM-2 and GSWM-3 are 0.5mm, 0.8mm and 1.2mm respectively. As per the manufacturer data sheet the tensile strength are in the range of 300-550 N/mm^2.

The mix proportion of mortar jacketing was 1:2 by weight of cement and sand, respectively. The water to cement ratio was 0.45. The compressive strength of mortar cube was 20.23 N/mm^2 and 32.65 N/mm^2 at 7 and 28 days of curing respectively.

3.7 Rehabilitation strategies

The repair consists of wrapping the damaged region using three types of GSWM and jacketed with mortar. The damaged control specimen S2 was rehabilitated using one layer of GSWM-1 and designated as RWM-1 while specimens S3 and S4 were rehabilitated using two layers of

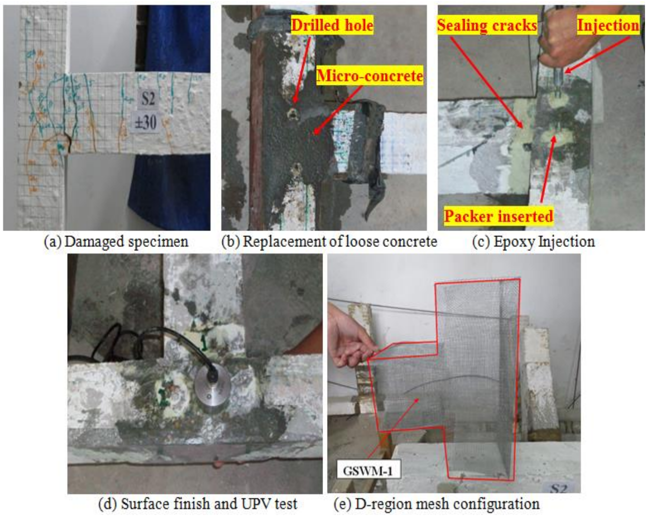

Fig. 6 Repair operation: treatment of affected zone

GSWM-2 and one layer of GSWM-3 respectively and was named as RWM2 and RWM3. Depending on the extent of damage GSWM were cut into a shape of D-region as defined by ACI 318-08 (2008) and typically shown in Fig. 6(e). The joints of the GSWM were secured at different locations together using double thin steel wires that are commonly used in tying reinforcing bars. Prior to wrapping of GSWM the affected zones were properly treated. Partial or complete replacement of loose concrete on the damaged area is necessary depending on the extent of damage and followed by epoxy resin injection. Prior to epoxy injection, the voids created after removal of loose materials were patched or filled with micro-concrete after a suitable bonding agent was applied on the clean surface for attaining adequate bond between old and freshly added concrete. Holes were drilled along cracks and packers were inserted through these holes, which served as filler neck for epoxy injection. Visible cracks were sealed and a low viscous epoxy resin was injected under high pressure into the cracked zone. Once the injected epoxy resin attained sufficient strength, the installed packers were removed and a grinding machine was subsequently used to remove the sealing materials. At 7 days of epoxy repairing all the sharp corner of the D-region of beam-column connection were rounded before placing of GSWM this is to facilitated stress reduction at the corners. Prior to wrapping of GSWM bonding agent was further applied on the surface of the concrete for attaining adequate bond between old concrete and freshly applied mortar. After bonding agent has been applied approximately 6 mm thick mix mortar of mixing ratio of 1:2 (cement: sand) by weight was placed on the surface of the specimens and then a wire mesh was wrapped around the joint and partly on beam and column as per the extent of damage. Thereafter, the specimens were further plastered about 6 mm thick with the same proportioned mix mortar. All jacketed specimens were cured for 28 days from the date of jacketing and then were tested under a similar cyclic loading to those of control specimens. Figs. 6 and 7 illustrates various steps of repair operations.

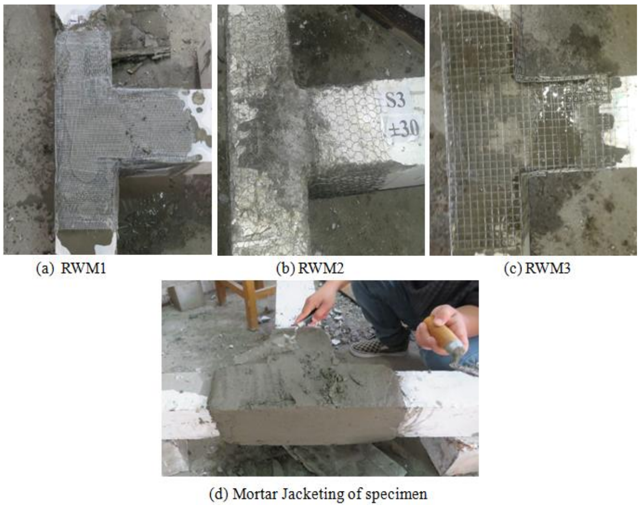

Fig. 7 Repair operation: confined using GSWM

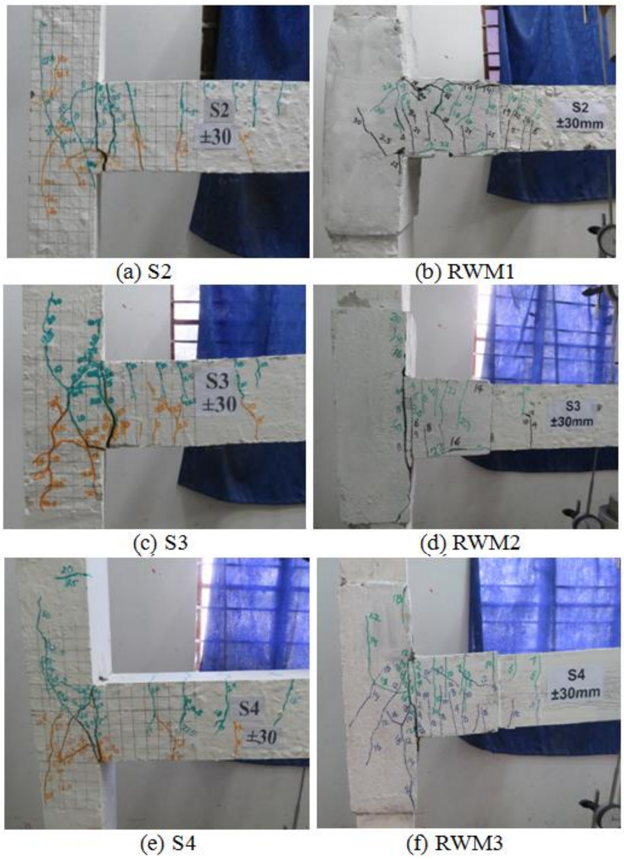

Fig. 8 Failure modes of RC beam-column connections

4. Behavior of RC beam-column connections: results and discussion

4.1 Failure mode of specimens

The failure modes and the extent of damage inflicted on the test specimens due to cyclic loading are presented in Fig. 8. In the early stage of cyclic loading, the first cracks in all the specimens mainly developed at the beam-column joint interface leading to the formation of a joint hinge.

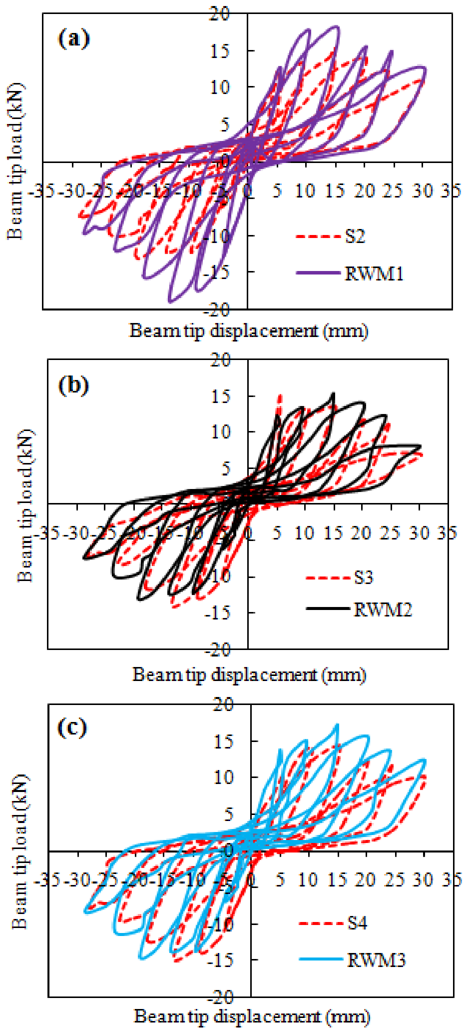

Fig. 9 Hysteretic responses

With further increase in loading, the cracks propagated towards their joint region or widening up the initial cracks at the joint face. A maximum crack width of about 5 mm was observed at the joint interface of control specimens. However, cracks in rehabilitated specimens were confined to the wire mesh jackets. It may be observed from the Fig. 8(b) that more number of cracks appeared in beam part of RWM1 with no wide cracks at joint region which indicates that GSWM-1 provided good bond resistance and ductility as compared to GSWM-2 and GSWM-1. Further, specimen wrapped with GSWM-1 delay the formation of plastic hinge as compared to other two specimen such failure pattern is a desirable failure modes for stability of an RC frame.

4.2 Hysteretic response of specimens

The typical hysteretic response obtained by plotting the test data is presented in Fig. 9. Various seismic parameters such as ultimate strength, energy dissipation, stiffness degradations and ductility of the specimens were evaluated from these hysteretic responses. Capacity comparison of specimens presented in Table 3 show marginally increase (+6%) in load carrying capacity, energy dissipation and ductility for RWM2 while a significant increase (+28%) for

Table 3 Capacity comparisons of RC beam-column connections

Specimens type	Average load capacity, kN (+ve and –ve)	Increase with respect to control specimen (%)	Energy dissipation (kN·mm)	Increase with respect to control specimen (%)	Ductility (d_u·d_y)	Increase with respect to control specimen (%)
S2	12.98	-	569	-	3.23	-
RWM1	16.58	28	754	33	4.82	49
S3	13.72	-	563	-	3.11	-
RWM2	14.75	8	594	6	3.35	8
S4	14.27	-	572	-	3.33	-
RWM3	16.95	19	658	15	4	20

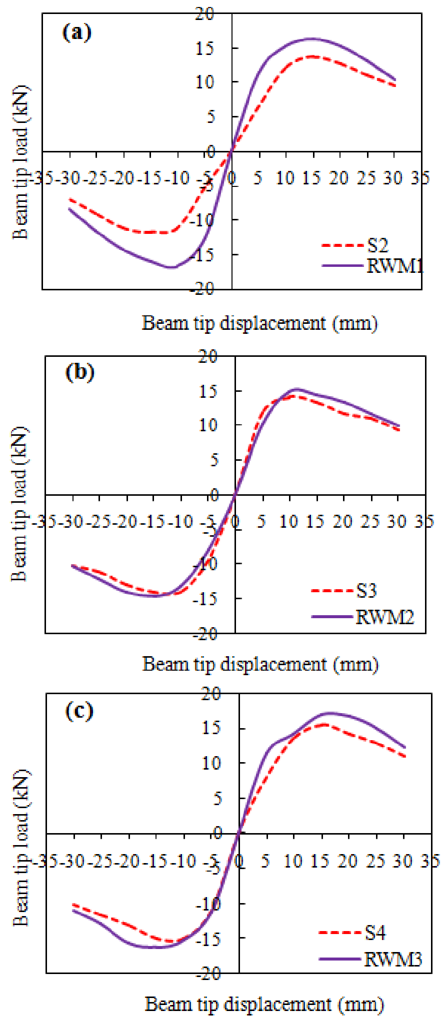

Fig. 10 Envelope curves

RWM1 followed by RWM3 (+15%) respectively as compared to control specimens. The behaviors of these connections were studied by comparing these parameters. Rehabilitated beam-column connections exhibited similar responses as compared to the control specimens. The envelope curves as obtained from hysteresis loops are shown in Fig. 10. Comparing these curves of (control and rehabilitated of corresponding specimens type) at each displacement, it can be observed that all the rehabilitated

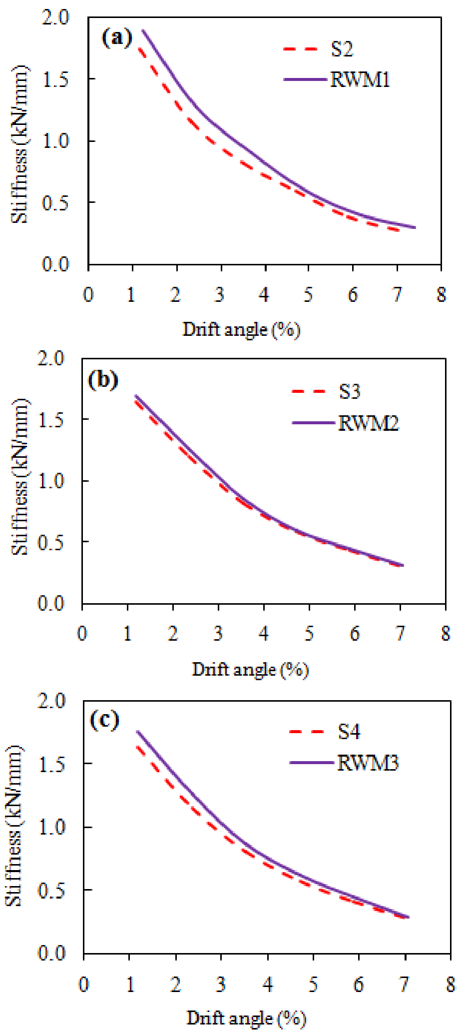

Fig. 11 Stiffness degradation

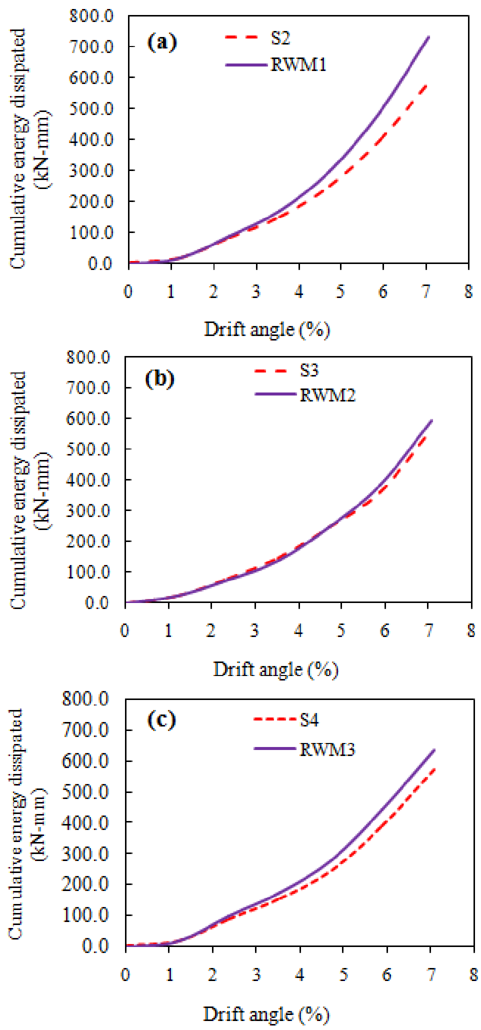

Fig. 12 Cumulative energy dissipation

specimens show a similar load displacement characterization with the initial slope being relatively lower. The envelope of hysteresis loops of the rehabilitated specimens, however, show higher load-carrying capacity in both push and pull directions except for specimen RWM2. Nevertheless, ultimate load carrying capacity of RWM2 is slightly higher (+8%) than the corresponding control specimens.

Thus, all damaged control specimens could successfully restored the load-carrying capacity after rehabilitation. This study shows that the appropriately chosen repair strategy could retrieve back the lost capacity of damaged structural component for post earthquake usage. Thus, it may be inferred that the applied repair techniques are effective in restoring the load-carrying capacity of the vital beam-column connections.

4.3 Stiffness degradation

Secant stiffness is evaluated as the peak-to-peak stiffness of the beam tip load-displacement relationship. The secant stiffness is an index of the response of the specimen during a cycle and its strength degradation from a cycle to the following cycle. It is calculated as the slope of the line joining the peak of positive and negative capacity at a given cycle. The slope of this straight line is the stiffness of the assemblage corresponding to that particular amplitude (Naeim and Kelly 1999). The typical stiffness degradation of the test specimens is presented in Fig. 11. Irrespective of the mesh types, they showed a similar degradation trend. Evaluating the reduction in stiffness of all the specimens it was observed that the degradation rate of stiffness is lower for RWM1 followed by RWM3 as compare to the corresponding control specimens S2 and S4 at the same displacement level. The lower degradation of stiffness is a desirable property in earthquake like situations. It was observed during the past earthquake that most of the RC structures failed due to sudden loss of stiffness with increasing lateral movement. In Fig. 11(b) stiffness degradation curves of RWM2 show equal or marginal lower as compared to S3. Therefore, from these comparisons it can be concluded that confinement of the damaged zone of RC beam-column connections using wire mesh lead to an enhancement of stiffness.

4.4 Cumulative energy dissipation

The performance of a structural element during seismic excitation depends to a large extent on its capacity to dissipate energy. The area of hysteresis loop is a measure of the energy dissipated. The cumulative energy dissipated at particular amplitude was calculated by summing up the energy dissipated in all the preceding cycles including that amplitude. The energy dissipation of specimens is presented in Table 3 and their variation with drift angle is presented in Fig. 12. As compared to their respective control specimens the increase in energy dissipation is about 33%, 6% and 15% for RWM1, RWM2 and RWM3 respectively. The increase in stiffness at the end of imposed displacement history attracted more load corresponding to any drift angle due to high strength epoxy resin injected into the damaged zone and mesh confinement, which prevent the initial crack propagations. Thus, the total area enclosed by the plot of beam tip load versus beam tip displacement was more. This was perhaps the reason for improvement in cumulative energy dissipation in the subsequent loading cycles.

4.5 Displacement ductility

The displacement ductility, which is the ratio between the ultimate displacements (d_u) to the displacement at first yield (d_y) was calculated for all the specimens following the method used by Shannag *et al*. (2005) which has been explained in Fig. 13. The ultimate displacement (d_u) was set at a displacement corresponding to 20% drop of peak load for computation. The yield displacement is calculated as the point of intersection between two straight lines drawn in the envelope curve. The first line is obtained by extending the line joining the origin and 50% of ultimate load capacity point on positive and negative sides of the envelope curve, while the second line is obtained by drawing a horizontal line through the 80% of ultimate load capacity point on either side. In the Fig. 13, d_{y1} and d_{y2} represent the yield displacement in positive and negative direction on the envelope curve respectively. The average value of yield displacement as obtained from both positive and negative direction is calculated. Horizontal lines drawn through the 80% of ultimate load capacity point on positive and negative side intersect the envelope curve at far end at points x_1 and x_2. The average of abscissa of these two points (denoted by d_{u1} and d_{u2} in Fig. 13) is taken as maximum displacement. The displacement ductility is calculated as the ratio of maximum displacement to the yield displacement and these values are presented in Table 3. Significant increases in ductility of the damaged connections due to confined GSWM-1 (49%) as compared to GWSM3 (20%). Nevertheless, rehabilitated specimens RWM2 are marginal higher (8%) than the control specimens which confirm the effectiveness of the repairing strategy.

4.6 Seismic damage index

Damage indices are intended to be used as numerical indicators of damage of any structural element under any loading type. Parameters such as strain, displacement, strength, energy and intrinsic dynamic properties are used to calculate these damage indices. The choice of an appropriate damage index may vary with the application.

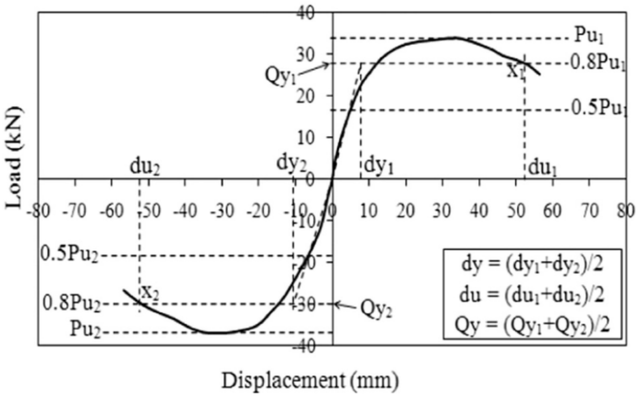

Fig. 13 Procedures for ductility calculation

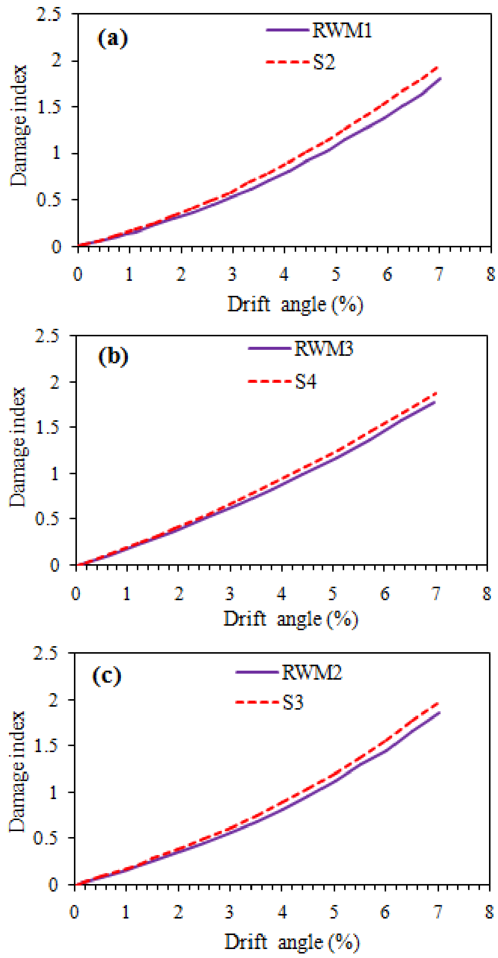

Fig. 14 Comparison of damage indices of the tested specimens

Williams and Sexsmith (1995) described Park and Ang (1985) damage index as the most accurate representation of damage development among all the available cumulative damage index models. This damage index model has been widely used in recent years because of its simplicity and more so due to the fact that it has been calibrated using experimental data from various structures damaged during the past earthquakes. Damage index model of Park and Ang (1985) as given in Eq. (1) was employ in this study in order to evaluate the damage level of the specimens.

$$DI = \frac{\delta_m}{\delta_u} + \frac{\beta}{\delta_u Q_y} \int dE \qquad (1)$$

where δ_m the maximum deflection attained during seismic loading, δ_u is the ultimate deflection capacity under monotonic load, Q_y is the yield force, dE is the incremental dissipated hysteretic energy and β is the strength degradation parameters. Parameters involved in the evaluation of the damage index were estimated as per Karayannis *et al*. (2008). The calculated damage indices for all specimens based on the above model are presented in Fig. 14. These figures show that the damage indices increase as the damage of specimens grow further with increased drift values. Further, all the curves of the damage indices are nearly linear, which suggest that the growth of damages in rehabilitated specimens is similar to the undamaged control specimens and the damage trends are stable. The lower damage index presented by rehabilitated indicated an effectiveness of the adopted rehabilitation strategy. Among the three type of mesh adopted, GSWM-1 suggested to be most promising in term of providing ductility to the RC beam-column connections.

4.7 Ultrasonic pulse velocity testing

Ultrasonic scanning is a recognized non destructive test method to assess the homogeneity and integrity of concrete structure. Assessment of control and rehabilitated specimens before and after rehabilitation using Ultrasonic Pulse Velocity (UPV) test were carried out and UPV values were used as indicators of damage status. It was observed that in most of the locations, the UPV values from the control specimen after damage were below 3.0 km/s. The UPV values below 3.0 km/s indicate that the qualities of the concrete at these zones are doubtful as per guidelines given by IS: 13311 (1992). However, after rehabilitations it has been observed that the UPV values improved considerably in the same location. Thus, it may be inferred that the cracks could be filled up by the injected epoxy. The UPV values after rehabilitation were above 3.3 km/s. Thus, it indicated that the quality of concrete fall in the good to excellent scale as per quality assessment guidelines. UPV tests were also done on the undamaged zone of each specimen for comparison purpose. Thus, this knowledge about the UPV values on the undamaged and damaged zones of control as well as rehabilitated specimen provided a very important platform for comparative analysis regarding the effectiveness of rehabilitation and also to reliably assess the condition of damaged concrete before rehabilitation.

4.8 Nominal principal tensile stresses

To have a better understanding of their behavior, nominal principal tensile stresses in beam-column joint region (damaged regions) were evaluated and compared in Fig. 15. From this figures it is can be deduced that the developed nominal principal tensile stresses of all control specimens are slightly lower than those of the rehabilitated specimens. However, the ability of high strength epoxy

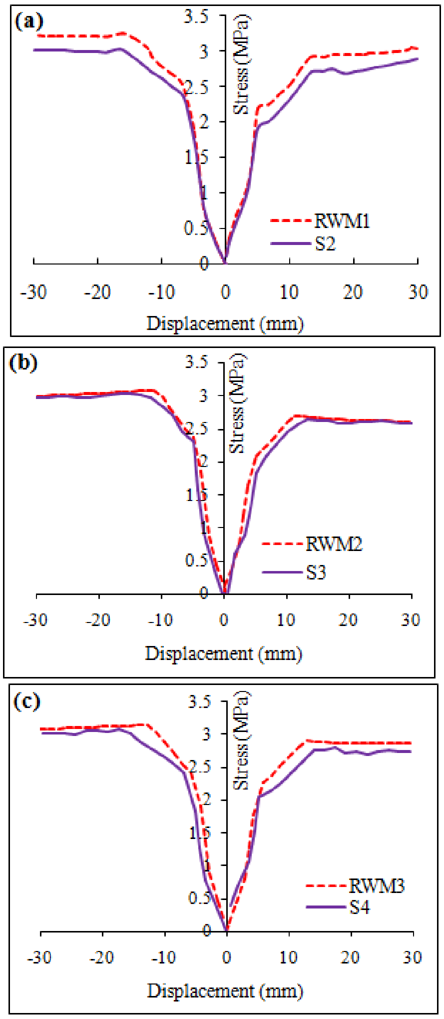

Fig. 15 Nominal principal tensile stress developed in beam-column joint region

resin confined with wire mesh jacket prevents the early crack initiation and crack propagation during cyclic loading; all rehabilitated specimens marginally increased the nominal principal tensile stresses of the damaged specimens. This shows the effectiveness of rehabilitation technique to restore the tensile stress of the damaged connections to the original state or even higher.

5. Conclusions

The damaged exterior RC beam-column connections were repair using epoxy resin injection and confined using three types of locally available galvanized steel wire mesh. The types of mesh chosen are based on the grid opening size and weaving types. Various parameters related to seismic capacity were evaluated and performances of these rehabilitated specimens were evaluated by comparing its results with those obtained from the respective control specimens. Based on experimental studies carried out, the following conclusions have been drawn.

• Comparison of important parameters related to seismic capacity such as ultimate load, stiffness degradation, energy dissipation, and ductility showed that the adopted rehabilitation strategies were satisfactory as damaged beam-column connections after rehabilitation exhibited equal or better performance. GSWM-1 and GSWM-3 significantly increases the seismic capacity of the damaged beam-column connection. Though, GSWM-2 did not show much improvement however, the lost capacity has been retrieved back to the original state.

• All rehabilitated specimens presented lower damage indices as compared to that of the corresponding control specimen.

• Nominal principal tensile stresses of rehabilitated specimens using GSWM-1 and GSWM-3 substantially increased in comparison to GSWM-2. Nevertheless, specimens rehabilitated using GSWM-2 is marginal higher than the control specimens.

• Among the three type of mesh adopted, GSWM-1 suggested to be most promising materials in term of providing ductility to the damaged RC beam-column connections.

• Finally, the results of this study show that lost capacity of the damaged specimens could be retrieved back to the original state or more using a combination of epoxy resin injection and wire mesh jacketing at modest costs. The results suggest that wire mesh is the most efficient and economic material for increasing the seismic capacity.

Acknowledgments

Authors are thankful to Mr. Babitdor Massar, Former JRF, Department of Civil Engineering, NIT Meghalaya for his help in casting, repairing and testing all the specimens.

References

ACI 318-08 (2008), Building Code Requirements for Structural Concrete and Commentary.

ACI 352R-02 (2002), Recommendations for Design of Beam-Column Connections in Monolithic Reinforced Concrete Structures, Farmington Hills, American Concrete Institute, MI.

ACI Com. 546 (1996), Concrete Repair Guide, Farmington Hills, ACI.

Alsayed, S.H., Al-Salloum, Y.A., Almusallam, T.H. and Siddiqui, N.A. (2010), "Seismic response of FRP-upgraded exterior RC beam-column joints", *J. Compos. Constr.*, ASCE, **14**(2), 195-208.

Applied Technology Council (1998), FEMA 308: Repair of Earthquake Damaged Concrete and Masonry Wall Buildings, Washington D.C., FEMA.

Ascione, F., Lamberti, M., Razaqpur, A.G. and Spadea, S. (2017), "Strength and stiffness of adhesively bonded GFRP beam-column moment resisting connections", *Compos. Struct.*, **60**, 1248-1257.

Bansal, P.P., Kumar, M. and Dar, M.A. (2016), "Retrofitting of exterior RC beam-column joints using ferrocement jackets", *Earthq. Struct.*, **10**(2), 313-328.

Bentayeb, F., Tahar, K.A. and Chateauneuf, A. (2008), "New technique for reinforcement of concrete columns confined by embedded composite grid", *Constr. Buld. Mater.*, **22**, 1624-1633.

Chidambaram, R.S. and Agarwal, P. (2014), "The confining effect of geo-grid on the mechanical properties of concrete specimens with steel fiber under compression and flexure", *Constr. Build. Mater.*, **71**, 628-637.

Choi, J.H. (2008), "Seismic retrofit of reinforced concrete circular columns using stainless steel wire mesh composite", *Can. J. Civil Eng.*, **35**(2), 140-147.

Corazao, M. and Durrani, A.J. (1989), "Repair and strengthening of beam-to-column connections subjected to earthquake loading", Technical Report NCEER-89-0013, National Center for Earthquake Engineering Research, State University of New York at Buffalo, N.Y.

Engindeniz, M., Kahn, L.F. and Zureick, A. (2005), "Repair and strengthening of reinforced concrete beam- column joints: State of the art", *ACI Struct. J.*, **102**(2), 187-197.

Esfahani, M.R., Kianoush, M.R. and Tajari, A.R. (2007), "Flexural behaviour of reinforced concrete beams strengthened by CFRP sheets", *Eng. Struct.*, **29**(10), 2428-2444.

Eslami, A. and Ronagh, H.R. (2014), "Experimental investigation of an appropriate anchorage system for flange-bonded carbon fiber-reinforced polymers in retrofitted RC beam-column joints", *J. Compos. Constr.*, **18**(4), 1-11.

Federal Emergency Management Agency (FEMA-308) (1998), Repair of Earthquake Damaged Concrete and Masonry Wall Buildings, 24-42.

Filiatrault, A. and Lebrun, I. (1996), "Seismic rehabilitation of reinforced concrete joints by epoxy pressure injection technique", *Spec. Publ.*, **160**, 73-92.

Ghobarah, A. and Said, A. (2002), "Shear strengthening of beam-column joints", *Eng. Struct.*, **24**(7), 881-888.

Ghobarah, A., Aziz, A. and Biddah, T.S. (1997), "Rehabilitation of reinforced concrete frame connections using corrugated steel jacketing", *ACI Struct. J.*, **4**(3), 283-294.

Hadi, M.N.S. and Tran, T.M. (2016), "Seismic rehabilitation of reinforced concrete beam-column joints by bonding with concrete covers and wrapping with FRP composites", *Mater. Struct.*, **49**(1-2), 467-485.

IS 10262 (2009), "Guidelines for concrete mix design proportioning (CED 2: Cement and Concrete)", Bureau of Indian Standard New Delhi.

IS 13311: Part 1(1992), Non-destructive Testing of Concrete: Part 1 Ultrasonic Pulse Velocity, Bureau of Indian Standard, New Delhi.

IS 13920 (2016), Ductile Detailing of Reinforced Concrete Structures Subjected to Seismic Forces-Code of Practice, Bureau of Indian Standard, New Delhi.

IS 1608 (1995), Mechanical Testing of Metals-Tensile Testing, Bureau of Indian Standard, New Delhi.

IS 432 1 (1982), Specification for Mild Steel and Medium Tensile Steel Bars and Hard-drawn Steel Wire for Concrete Reinforcement: Part I Mild Steel and Medium Tensile Steel Bars, Bureau of Indian Standard, New Delhi.

IS 456 (2000), Plain and Reinforced Concrete-Code of Practice, Bureau of Indian Standard, New Delhi.

Kakaletsis, D.J., David, K.N. and Karayannis, C.G. (2011), "Effectiveness of some conventional seismic retrofitting techniques for bare and infilled R/C frame", *J. Struct. Eng. Mech.*, **39**(4), 499-520.

Karayannis, C.G. and Sirkelis, G.M. (2002), "Effectiveness of RC beam-column connection strengthening using Carbon-FRP Jackets", *12th European Conference on Earthquake Engineering*, London, Paper No. 546.

Karayannis, C.G. and Sirkelis, G.M. (2008), "Strengthening and rehabilitation of RC beam-column joints using C-FRP jacketing and epoxy resin injection", *J. Earthq. Eng. Struct. Dyn.*, **37**,

769-790.
Karayannis, C.G., Chalioris, C.E. and Sideris, K.K. (1998), “Effectiveness of RC beam-column connection repair using epoxy resin injections”, *J. Earthq. Eng.*, **2**(2), 217-240.
Karayannis, C.G., Chalioris, C.E. and Sirkelis, G.M. (2008), “Local retrofit of exterior RC beam-column joints using thin RC jackets-An experimental study”, *Earthq. Eng. Struct. Dyn.*, **37**, 727-746.
Kumar, V. and Patel, P.V. (2016), “Strengthening of axially loaded circular concrete columns using stainless steel wire mesh (SSWM)-Experimental investigations”, *Constr. Build. Mater.*, **124**, 186-198.
Li, B., Lam, E.S., Wu, B. and Wang, Y. (2015), “Seismic behavior of reinforced concrete exterior beam-column joints strengthened by ferrocement composites”, *Earthq. Struct.*, **9**(1), *233-256.*
Marthong, C., Dutta, A. and Deb, S.K. (2013), “Seismic rehabilitation of RC exterior beam-column connections using epoxy resin injection”, *J. Earthq. Eng.*, **17**(3), 378-398.
Mosallam, A.S. (2000), “Strength and ductility of reinforced concrete moment frame connections strengthened with quasi-Isotropic laminates”, *Compos. Part B-Eng.*, **31**(6-7), 481-497.
Mukherjee, A. and Joshi, M. (2005), “FRPC reinforced concrete beam-column joints under cyclic excitation”, *Compos. Struct.*, **70**, 185-199.
Naeim, F. and Kelly, J.M. (1999), *Design of Seismic Isolated Structures from Theory to Practice*, John willey & sons, inc.
Park, Y.J. and Ang, A.H.S. (1985), “Mechanistic seismic damage model for reinforced concrete”, *J. Struct. Eng.*, **111**(4), 722-739.
Patel, P.V., Raiyani, S.D. and Shah, P.J. (2018), “Torsional strengthening of RC beams using stainless steel wire mesh - Experimental and numerical study”, *Struct. Eng. Mech.*, **67**(4), 391-401.
Saleh, H.A., Al-Salloum, A.Y., Almusallam, T.H. and Nadeem, A.S. (2010), “Seismic response of FRP-upgraded exterior beam-column joints”, *J. Compos. Constr.*, ASCE, **14**(2), 195-208.
Shannag, M.J. and Alhassan, M.A. (2005), “Seismic upgrade of interior beam-column sub-assemblages with high performance fiber reinforced concrete jackets”, *ACI Struct. J.*, **102**(1), 131-138.
Silva, M.F.A. and Haach, V.G. (2016), “Parametrical study of the behavior of exterior unreinforced concrete beam-column joints through numerical modeling”, *Comput. Concrete*, **18**(2), 215-233.
Teng, J.G., Chen, J.F., Smith, S.T. and Lam, L. (2002), *FRP-Strengthened RC Structures*, John Wiley & Sons, Ltd.
Tsai, A. (1992), “Effective repair with resin for bond failure of RC members”, *Proceedings of the 10th World Conference of Earthquake Engineering*, 5211-5216.
Tsonos, A.G. (2008), “Effectiveness of CFRP-jackets and RC-jackets in post-earthquake and pre-earthquake retrofitting of beam-column sub-assemblages”, *Eng. Struct.*, **30**, 777-793.
Tsonos, A.G. (2010), “Performance enhancement of R/C building columns and beam-column joints through shotcrete jacketing”, *Eng. Struct.*, **32**, 726-740.
Tsonos, A.G. (2014), “An innovative solution for strengthening of old R/C structures and for improving the FRP strengthening method”, *Struct. Monit. Mainten.*, **1**(3), 323-338.
Tsonos, A.G. and Papanikolaou, K.V. (2003), “Post-earthquake repair and strengthening of RC beam column connections (theoretical & experimental investigation)”, *Bull. NZ Soc. Earthq. Eng.*, **36**(2), 73-79.
Vidjeapriya, R. and Jaya, K.P. (2013), “Experimental study on two simple mechanical precast beam-column connections under reverse cyclic loading”, *J. Perform. Constr. Facil.*, **27**(4), 402-414.
William, M.S. and Sexsmith, R.G. (1995), “Seismic damage indices for concrete structures: a state-of-the-art review”, *Earthq. Spectra*, **11**(2), 319-349.

AT